Published in final edited form as:
J Proteome Res. 2011 December 2; 10(12): 5463–5471. doi:10.1021/pr200718p.

Quantitative Proteomic Analysis Revealed Lovastatin-induced Perturbation of Cellular Pathways in HL-60 Cells

Xiaoli Dong, **Yongsheng Xiao**, **Xinning Jiang**, and **Yinsheng Wang***
Department of Chemistry, University of California, Riverside, California 92521-0403

Abstract

Lovastatin, a member of the statin family of drugs, is widely prescribed for treating hypercholesterolemia. Statin family of drugs, however, also show promise for cancer treatment and prevention. Although lovastatin is known to be an inhibitor for HMG-CoA reductase, the precise mechanisms underlying the drug's antiproliferative activity remain unclearly defined. Here we utilized mass spectrometry, in conjunction with stable isotope labeling by amino acids in cell culture (SILAC), to analyze the perturbation of protein expression in HL-60 cells treated with lovastatin. We were able to quantify ~3200 proteins with both forward and reverse SILAC labeling experiments, among which ~120 exhibited significant alterations in expression levels upon lovastatin treatment. Apart from confirming the expected inhibition of cholesterol biosynthesis pathway, our quantitative proteomic results revealed that lovastatin perturbed estrogen receptor signaling pathway, which was manifested by the diminished expression of estrogen receptor α, steroid receptor RNA activator 1 and other related proteins. Lovastatin also altered glutamate metabolism through down-regulation of glutamine synthetase and γ-glutamylcysteine synthetase. Moreover, lovastatin treatment led to a marked down-regulation of carbonate dehydratase II (a.k.a. carbonic anhydrase II) and perturbed the protein ubiquitination pathway. Together, the results from the present study underscored several new cellular pathways perturbed by lovastatin.

Keywords

Lovastatin; HL-60 cell; SILAC; estrogen receptor; carbonate dehydratase II

Introduction

Lovastatin is a widely prescribed cholesterol-lowering drug and it inhibits 3-hydroxy-3-methylglutaryl-coenzyme A (HMG-CoA) reductase, which converts HMG-CoA to mevalonate and is a key regulatory enzyme in cholesterol biosynthesis. The end products of the mevalonate pathway are required for a number of essential cellular functions including membrane integrity and steroid production, electron transfer and cell respiration, covalent binding of proteins to membranes, etc.[1–3] HMG-CoA reductase inhibitors have been shown to inhibit cellular proliferation and induce apoptosis in several experimental settings, thus rendering them promising agents for cancer treatment and prevention.[3–5] However, the detailed molecular mechanisms underlying the antitumor activity of lovastatin remain poorly defined.

*To whom correspondence should be addressed: Phone: (951) 827-2700. Fax: (951) 827-4713. yinsheng.wang@ucr.edu.

Supporting Information Available: Tables for results from protein identification and quantification. This material is available free of charge via the Internet at http://pubs.acs.org.

With the recent advances in instrumentation, mass spectrometry (MS)-based proteomics now allows for the identification and quantification of thousands of proteins in complex samples. A variety of stable-isotope labeling strategies, such as isotope-coded affinity tag (ICAT),[6] isobaric tags for relative and absolute quantitation (iTRAQ)[7] and stable-isotope labeling by amino acids in cell culture (SILAC),[8] have been developed for the quantitative analysis of differential protein expression. Among these isotope-labeling strategies, SILAC, as a metabolic labeling method, is simple, efficient, and can allow for almost complete heavy isotope incorporation. With the use of SILAC, accurate results could be obtained with minimal bias, thereby facilitating relative quantification of subtle changes in protein abundance.[8]

Previous studies revealed that cultured acute myelocytic leukemia (AML) cells exhibited significant sensitivity to lovastatin-induced apoptosis,[9] and the apoptosis induction in HL-60 cells involves inhibition of Na^+/H^+ antiporter.[10] The latter inhibition results in a reduction of intracellular pH and induces DNA degradation.[10] The upstream events leading to the inhibition of Na^+/H^+ antiporter, however, remain unclear.

To explore novel mechanisms underlying the anticancer activity of lovastatin in leukemia cells, we employed LC-MS/MS, along with SILAC, to assess quantitatively the drug-induced perturbation of protein expression in HL-60 human acute promyelocytic leukemia (APL) cells. More than 3000 proteins were quantified in both forward and reverse SILAC measurements, among which 122 were significantly altered upon lovastatin treatment. Importantly, we observed, for the first time, the lovastatin-induced down-regulation of glutamate synthetase, carbonate dehydratase II, ERα and SRA, which may contribute to the cytotoxic effects of lovastatin.

Materials and Methods

Materials

All reagents unless otherwise stated were from Sigma (St. Louis, MO). Heavy lysine and arginine ($[^{13}C_6,^{15}N_2]$-L-lysine and $[^{13}C_6]$-L-arginine) were purchased from Cambridge Isotope Laboratories (Andover, MA).

Cell culture

HL-60 cells, obtained from ATCC (Manassas, VA), were cultured in Iscove's modified minimal essential medium (IMEM) supplemented with 10% fetal bovine serum (FBS, Invitrogen, Carlsbad, CA) and penicillin (100 IU/mL). Cells were maintained in a humidified atmosphere with 5% CO_2 at 37°C, with medium renewal at every 2 or 3 days depending on cell density. For SILAC experiments, the IMEM medium without L-lysine or L-arginine was custom-prepared according to ATCC formulation. The complete light and heavy IMEM media were prepared by the addition of light or heavy lysine and arginine, along with dialyzed FBS, to the above lysine, arginine-depleted medium. The HL-60 cells were cultured in heavy IMEM medium for at least 5 cell doublings to achieve complete isotope incorporation as described by Mann et al.[8]

Lovastatin treatment and cell lysate preparation

In forward SILAC experiment, HL-60 cells, cultured in light medium, at a density of approximately 7.5×10^5 cells/mL were treated with 10 μM lovastatin for 24 h, whereas the cells cultured in heavy medium were untreated. Reverse SILAC experiments were also performed in which the cells cultured in the heavy and light medium were treated with lovastatin and mock-treated, respectively (Figure 1). After 24 h, the light and heavy isotope-

labeled cells were collected by centrifugation at 300 g and washed three times with ice-cold PBS.

The cell pellets were then resuspended in CelLytic^{TM} M cell lysis reagent for 30 min with occasional vortexing. Cell lysates were centrifuged at 12,000 g at 4°C for 30 min and the resulting supernatants collected. To the supernatant was subsequently added a protease inhibitor cocktail, and the protein concentrations of the cell lysates were determined by using Quick Start Bradford Protein Assay kit (Bio-Rad, Hercules, CA).

SDS-PAGE separation and in-gel digestion

The light and heavy cell lysates were combined at 1:1 ratio (w/w), denatured by boiling in Laemmli loading buffer for 5 min and separated by 12% SDS-PAGE with a 4% stacking gel. The gel was stained with Coomassie blue; after destaining, the gel was cut into 20 bands, in-gel reduced with dithiothreitol and alkylated with iodoacetamide. The proteins were digested in-gel with trypsin (Promega, Madison, WI) for overnight, after which peptides were extracted from gels with 5% acetic acid in H_2O and then with 5% acetic acid in CH_3CN/H_2O (1:1, v/v). The resulting peptide mixtures were dried and stored at −20°C until further analysis.

LC-MS/MS for protein identification and quantification

On-line LC-MS/MS analysis was performed on an LTQ-Orbitrap Velos mass spectrometer coupled with EASY n-LCII and a nanospray source (Thermo, San Jose, CA). The HPLC separation was carried out using a home-made trapping column (150 μm×50 mm) and a separation column (75 μm×120 mm). Both the trapping and separation columns were packed with ReproSil-Pur C18-AQ resin (5 μm in particle size, Dr. Maisch HPLC GmbH, Germany). The peptide mixture was first loaded onto the trapping column with a solvent mixture of 0.1% formic acid in CH_3CN/H_2O (2:98, v/v) at a flow rate of 4.0 μL/min. The peptides were then separated with a 120-min linear gradient of 2–40% acetonitrile in 0.1% formic acid and at a flow rate of 300 nL/min.

The LTQ-Orbitrap Velos mass spectrometer was operated in the positive-ion mode, and the spray voltage was 1.8 kV. All MS/MS spectra were acquired in a data-dependent scan mode, where one full MS scan was followed with twenty MS/MS scans. The full-scan mass spectra (from *m/z* 350 to 2000) were acquired with a resolution of 60,000 at *m/z* 400 after accumulation to a target value of 500,000. The twenty most abundant ions found in MS at a threshold above 500 counts were selected for fragmentation by collision-induced dissociation at a normalized collision energy of 35%.

Data processing

Maxquant, Version B.01.03, was used to identify and quantify the global proteomes.[11] The maximum number of miss-cleavages for trypsin was two per peptide. Cysteine carbamidomethylation and methionine oxidation were set as fixed and variable modifications, respectively. The tolerances in mass accuracy for MS and MS/MS were 25 ppm and 0.6 Da, respectively. Maximum false discovery rates (FDRs) were set to 0.01 at both peptide and protein levels, and minimum required peptide length was six amino acids. SILAC quantification setting was adjusted to doublets, with lysine (+8 Da) and arginine (+6 Da) being selected as heavy labels. Only proteins with at least two peptides were considered as reliably identified. Peptides were considered for quantification with a minimum ratio count of 2.[12] Proteins with significant changes in SILAC experiments were determined by a combination of ratio and ratio significance calculated by MaxQuant. The p-value for the significance of enrichment was set to be <0.01 in both forward and reverse SILAC labeling experiments. The quantification was based on three independent SILAC and LC-MS/MS

experiments, which included two forward and one reverse SILAC labelings, and the proteins reported here could be quantified in both forward and reverse SILAC experiments.

Results and Discussion

Lovastatin treatment, protein identification and quantification

To gain insights into the molecular pathways perturbed by lovastatin treatment, we employed SILAC in conjunction with LC-MS/MS to assess the lovastatin-induced differential expression of the whole proteome of HL-60 cells. To perform proteomic experiments with the optimal dose of lovastatin, the dose-dependent survival rate of HL-60 cells upon lovastatin treatment was initially determined. Based on trypan blue exclusion assay, a less than 5% cell death was observed after a 24-hr treatment with 10 μM lovastatin, whereas a significant reduction in cell viability (by ~25%) was induced by a 24-hr treatment with 20 μM lovastatin. Thus, we chose 10 μM lovastatin for subsequent experiments to minimize the apoptosis-induced alteration in protein expression.

HL-60 cells were cultured in both light and heavy media. After treatment with lovastatin, the cells were lysed, and the lysates were combined and subsequently fractionated by SDS-PAGE. After in-gel digestion, the proteins were identified and quantified by LC-MS/MS. To obtain reliable quantification results, we conducted SILAC experiments in triplicate, with two sets of forward and one set of reverse labelings (Figure 1 and the Materials and Methods section). A total of 3228 proteins were identified and quantified from lovastatin-treated or untreated sample. Details of all quantified proteins can be found in supplemental Table S1.

For screening the significantly changed proteins, we considered only the quantification results for those proteins that could be quantified in all three experiments or in two experiments, which included both the forward and reverse SILAC labelings. Figure 2 depicts the representative MS quantification result of peptide LLLTLPLLR from estrogen receptor α (ERα). As can be seen, in both forward and reverse SILAC experiments, this peptide showed significant down-regulation upon treatment with lovastatin, supporting the down-regulation of the protein from which the peptide is derived (Figure 2A&B). In addition, the MS/MS results revealed the unambiguous identification of this peptide (Figure 2C&D).

The distribution of changes in protein expression levels arising from lovastatin treatment is displayed in Figure 3. Among the 3228 quantified proteins, most did not exhibit significant changes. The average ratio and the average relative standard deviation (RSD) of ratios for all quantified proteins were ~1.0 and 20%, respectively. Thus, a ratio of > 1.5 or < 0.67 was selected as threshold for screening the significantly changed proteins.[13, 14] It turned out that a total of 122 proteins displayed significant changes upon lovastatin treatment, among which 42 and 80 were up- and down-regulated, respectively. The quantification results for the proteins with significant changes are summarized in Table 1 and the detailed protein identification information can be found in Table S1.

Lovastatin perturbed cholesterol biosynthesis pathway

Lovastatin is an inhibitor for HMG-CoA reductase, an enzyme that catalyzes the conversion of HMG-CoA to mevalonate, which is a key intermediate in cholesterol biosynthesis. Thus, lovastatin inhibits the endogenous production of cholesterol. Both lymphocytes and leukemia cells rely on endogenously synthesized cholesterol for proliferation; specific inhibition of endogenous cholesterol biosynthesis, despite the presence of exogenous cholesterol in the serum-containing growth medium, leads to growth inhibition.[3, 15] Along this line, we found that treatment with 10 μM lovastatin resulted in a less than 20% increase

in cell population in 24 hrs, which is much lower than that observed for the untreated cells, whose population was doubled in 24 hrs.

Our LC-MS/MS quantification results revealed that HMG-CoA synthase and farnesyl diphosphate (FDP) synthase were reduced by approximately 50% upon lovastatin treatment. Both enzymes are required for the biosynthesis of cholesterol from acetoacetyl-CoA in human cells.[16] Our quantitative proteomic results, therefore, confirm that cholesterol biosynthesis pathway was perturbed by lovastatin treatment. These results also underscored that the SILAC-based quantitative proteomic method can provide an accurate assessment of lovastatin-induced alteration in protein expression levels.

Lovastatin induced the down-regulation of estrogen receptor α (ERα), steroid receptor RNA activator 1 (SRA) and other proteins in ER signaling pathway

The LC-MS/MS quantification results showed that ERα, SRA, general transcription factor TFIIB, adenylate kinase isoenzyme 6 (TAF9), activator-recruited cofactor 205 kDa component (MED1) and activator-recruited cofactor 240 kDa component (MED12) were down-regulated by approximately 30% upon lovastatin treatment (Table 1 and Table S2). These proteins are involved in estrogen receptor signaling in human cells, with ERα being the final target in this pathway. SRA is able to augment the estradiol-induced gene transcription through ERα and ERβ.[17] Breast cancer patients with high level of SRA expression had a significantly worse survival rate than those with low SRA levels; thus, SRA expression may serve as a new prognosis marker for patients with ER-positive breast tumors.[18]

Approximately 70% of breast cancer cases have an overexpression of estrogen receptors, which are referred to as “ER-positive”, and HL-60 cells are also ER-positive.[19] Estrogen binding to ER stimulates proliferation of mammary cells, and estrogen metabolism also induces DNA damage.[20] Both processes may ultimately result in tumor formation; therefore, ER antagonists are currently used for breast cancer treatment.[21] Recent clinical data showed that statins may influence the phenotype of breast tumors, suggesting a new potential strategy for breast cancer prevention, namely, by combining statins with other agents (e.g. tamoxifen, aromatase inhibitors).[22] Our quantitative proteomic data showed that treatment of HL-60 cells with 10 μM lovastatin for 24 hrs led to an ~35% decline in expression levels of ERα and SRA. This represents the first finding that lovastatin can induce reduction in expression levels of ERα and SRA in leukemia cells, which may contribute to lovastatin-mediated growth inhibition of HL-60 cells.

Carbonate dehydratase II (CAII) was significantly down-regulated by lovastatin treatment

CAII is a predominant enzyme catalyzing the reversible hydration of carbon dioxide to bicarbonate and proton, which facilitates pH homeostasis in blood and other tissues.[23] Leppilampi et al.[24] showed that many AML cell lines, including the HL-60 cells, express CAII. The presence of CAII in leukemia cells suggests that it may participate in the regulation of pH homeostasis in these cells. In addition, tumor cells require high bicarbonate flux for growth, rendering inhibition of CAII a promising strategy for cancer treatment.[24] We found that lovastatin induced a marked reduction (by ~ 6 fold, Table 1) in expression level of CAII, suggesting that the drug-induced growth inhibition of HL-60 cells may emanate partly from the diminished expression of CAII.

Lovastatin is also known to inhibit Na^+/H^+ exchanger (NHE), which regulates acid-base homeostasis as well as growth and invasion of cancer cells.[24] NHE inhibition gives rise to elevated intracellular pH which can induce DNA degradation.[10, 25] Moreover, CAII could bind to and enhance the activity of NHE, and treatment with CAII inhibitor acetazolamide

significantly reduced NHE activity.[26, 27] Therefore, the down-regulation of CAII may constitute an important upstream event leading to the lovastatin-induced decline in Na^+/H^+ exchange that was previously observed.[10]

It is interesting to note that mRNA levels of both CAII and NHE 3 mRNA were decreased in efferent ductules of male ER-knockout mice.[28] Additionally, several estrogen derivatives, including estrone 3-*O*-sulfamate (EMATE) which is a potent irreversible inhibitor of steroid sulfatase, are also highly active reversible inhibitors of CAII.[29] Thus, the relationship between ER, CAII and NHE may be established, where CAII can alter the activity of NHE, and ER can regulate the levels of both CAII and NHE, as depicted in Figure 4. In keeping with this notion, ER level was also down-regulated by lovastatin treatment (*vide supra*).

Lovastatin induced the alteration in expression of other important enzymes

We next conducted protein interaction network and pathway analysis using the Ingenuity Pathway Analysis (IPA) software.[30] Proteins with greater than a 1.5-fold change in expression upon the drug treatment were included for the analysis. Networks represent a highly interconnected set of proteins derived from the input data set. Biological functions and processes were assigned to networks by mapping the proteins in the network to functions in the Ingenuity ontology. Pathways found to be altered included glutamate metabolism, protein ubiquitination pathway, and EIF2 signaling, *etc.* (Table 2).

Glutamine synthetase (GS) and γ-glutamylcysteine synthetase (γ-ECS) are involved in glutamate metabolic pathway. GS catalyzes the conversion of glutamic acid (Glu) to glutamine, and B lymphoblastoid cells, including HL-60 cells, are highly dependent on glutamine.[31] We observed that GS was decreased by nearly 60% upon lovastatin treatment in HL-60 cells, which is in keeping with Tsai's finding in hippocampal astrocytes with cholesterol deprivation as validated by Western-blot.[32] Together, we conclude that the lovastatin-induced growth inhibition of HL-60 cells may arise partly from glutamine deficiency. γ-ECS, which employs glutamate and cysteine as substrates, is the first enzyme in the glutathione biosynthesis pathway. High level of γ-ECS and glutathione could protect AML cells against etoposide-induced apoptosis.[33] We found that γ-ECS level was decreased by 35% upon lovastatin treatment, which may lead to elevated oxidative stress in HL-60 cells.

We also observed that many proteins involved in the ubiquitination pathway were down-regulated upon lovastatin treatment. These include the non-canonical ubiquitin-conjugating enzyme 1 (UBE2J1), ubiquitin-conjugating enzyme E2 S (UBE2S), DNAJ homolog subfamily C member 2 (DNAJC2), deubiquitinating enzyme 10 (USP10), baculoviral IAP repeat-containing protein 6 (BIRC6) and cDNA FLJ54183, highly similar to HLA class I histocompatibility antigen, and Cw-7 α chain (HLA-C, Table 1 and Table S2). The ubiquitination system functions in a wide variety of cellular processes including cell cycle progression. In this context, destruction of regulatory proteins via ubiquitin-dependent proteasomal pathway is a major and essential mechanistic step in various aspects of cell cycle control. Cyclin-dependent kinases (CDKs) and cyclins are major control switches for cell cycle progression and they cause the cells to transit from G1 to S and from G2 to M phases. Proteolytic degradation is required for removing proteins that function as CDK inhibitors.[34] From our proteomics study, both cell division cycle 2-like protein kinase 1 (a.k.a. cyclin-dependent kinase; CDK1) and ubiquitination pathway-related proteins were decreased by ~30% (Table S2). Thus, CDK activity might be modulated by CDK inhibitors since proteasomal degradation of these proteins might be compromised. Along with the decreased expression of other cell cycle-associated proteins, including G1-to-S phase transition protein 1, cell division cycle protein 123 homolog and cell proliferation-inducing

gene 50 protein (Table 1), we deduce that lovastatin may induce growth inhibition through perturbation of cell cycle progression.

Aside from the significant decline in expression of the aforementioned proteins, lovastatin treatment also led to a systematic down-regulation of several important groups of proteins involved in translation (Table 1). In this context, translation elongation factors were all modestly down-regulated upon lovastatin treatment (Table S3). These results are in accordance with the lovastatin-induced growth inhibition of HL-60 cells (see above).

Conclusions

Lovastatin has shown great promise for cancer prevention and treatment.[3–5] The molecular mechanisms contributing to the antineoplastic effects of lovastatin, however, remain not well established. In this study, we provided a proteomic description of lovastatin-induced cellular alterations in a widely studied leukemia cell line. Our results revealed that the drug treatment of HL-60 cells led to the up- or down-regulation of many important proteins, including carbonate dehydratase II, estrogen receptor α, glutamate synthetase, HMG-CoA synthase, *etc*. In addition, most translation elongation factors were modestly down-regulated upon the treatment.

Among the proteins whose expression was perturbed by lovastatin, the down-regulation of ERα and SRA, which were essential components in the ER signaling pathway,[17] are of particular importance. Our data revealed that both ERα and SRA were down-regulated upon lovastatin treatment. On the grounds that the HL-60 cells are ER-positive, the compromised ER signaling may contribute to the cytotoxic effects of lovastatin in HL-60 cells. We also observed that the expression level of CAII was substantially decreased upon lovastatin treatment, which could be attributed in part to the down-regulation of ER viewing that the level of CAII was known to be a target for ER signaling.[28] Thus, the findings made from the present quantitative proteomic study, together with previous observation that CAII is known to bind and enhance the activity of Na^+/H^+ exchanger,[26] provide novel mechanistic insight about the upstream events leading to previously observed perturbation in intracellular pH homeostasis in HL-60 cells induced by lovastatin treatment.[10] Moreover, lovastatin induced the reduction in the expression level of GS, which could result in glutamine depletion; this may constitute another important pathway leading to growth inhibition.

The current study improves our understanding of mechanisms of lovastatin-induced anticancer effect, and confirms that the SILAC-based quantitative proteomic analysis is a powerful tool for unveiling alterations in protein expression arising from treatment of an antitumor drug (*i.e.*, lovastatin). This approach opens the door for discovering novel molecular pathways perturbed by lovastatin treatment and affords potential new therapeutic targets for the treatment of APL and other human cancers.

Supplementary Material

Refer to Web version on PubMed Central for supplementary material.

Acknowledgments

This work was supported by the National Institutes of Health (R01 CA 116522).

Abbreviations

APL	acute promyelocytic leukemia

ERα	estrogen receptor α
FDP synthase	farnesyl diphosphate synthase
hnRNP	heterogeneous nuclear ribonuclear protein
HMG-CoA	3-hydroxy-3-methylglutaryl-CoA
MS	mass spectrometry
SILAC	stable isotope labeling by amino acids in cell culture
SRA	steroid receptor RNA activator 1

References

1. Goldstein JL, Brown MS. Regulation of the mevalonate pathway. Nature. 1990; 343:425–430. [PubMed: 1967820]
2. Etienne-Manneville S, Hall A. Rho GTPases in cell biology. Nature. 2002; 420:629–635. [PubMed: 12478284]
3. Wong WW, Dimitroulakos J, Minden MD, Penn LZ. HMG-CoA reductase inhibitors and the malignant cell: the statin family of drugs as triggers of tumor-specific apoptosis. Leukemia. 2002; 16:508–519. [PubMed: 11960327]
4. Chan KK, Oza AM, Siu LL. The statins as anticancer agents. Clin Cancer Res. 2003; 9:10–19. [PubMed: 12538446]
5. Demierre MF, Higgins PD, Gruber SB, Hawk E, Lippman SM. Statins and cancer prevention. Nat Rev Cancer. 2005; 5:930–942. [PubMed: 16341084]
6. Gygi SP, Rist B, Gerber SA, Turecek F, Gelb MH, Aebersold R. Quantitative analysis of complex protein mixtures using isotope-coded affinity tags. Nat Biotech. 1999; 17:994–999.
7. Ross PLHYN, Marchese JN, Williamson B, Parker K, Hattan S, Khainovski N, Pillai S, Dey S, Daniels S, Purkayastha S, Juhasz P, Martin S, Bartlet-Jones M, He F, Jacobson A, Pappin DJ. Multiplexed protein quantitation in Saccharomyces cerevisiae using amine-reactive isobaric tagging reagents. Mol Cell Proteomics. 2004; 3:1154–1169. [PubMed: 15385600]
8. Ong SE, Blagoev B, Kratchmarova I, Kristensen DB, Steen H, Pandey A, Mann M. Stable isotope labeling by amino acids in cell culture, SILAC, as a simple and accurate approach to expression proteomics. Mol Cell Proteomics. 2002; 1:376–386. [PubMed: 12118079]
9. Dimitroulakos J, Nohynek D, Backway KL, Hedley DW, Yeger H, Freedman MH, Minden MD, Penn LZ. Increased sensitivity of acute myeloid leukemias to lovastatin-induced apoptosis: A potential therapeutic approach. Blood. 1999; 93:1308–1318. [PubMed: 9949174]
10. Perezsala D, Colladoescobar D, Mollinedo F. Intracellular alkalinization suppresses lovastatin-induced apoptosis in HL-60 cells through the inactivation of a pH-dependent endonuclease. J Biol Chem. 1995; 270:6235–6242. [PubMed: 7890761]
11. Cox J, Mann M. MaxQuant enables high peptide identification rates, individualized p.p.b.-range mass accuracies and proteome-wide protein quantification. Nat Biotechnol. 2008; 26:1367–1372. [PubMed: 19029910]
12. Argenzio E, Bange T, Oldrini B, Bianchi F, Peesari R, Mari S, Di Fiore PP, Mann M, Polo S. Proteomic snapshot of the EGF-induced ubiquitin network. Mol Syst Biol. 2011; 7:462. [PubMed: 21245847]
13. Yu KH, Barry CG, Austin D, Busch CM, Sangar V, Rustgi AK, Blair IA. Stable Isotope Dilution Multidimensional Liquid Chromatography-Tandem Mass Spectrometry for Pancreatic Cancer Serum Biomarker Discovery. J Proteome Res. 2009; 8:1565–1576. [PubMed: 19199705]
14. Xiong L, Wang YS. Quantitative proteomic analysis reveals the perturbation of multiple cellular pathways in HL-60 cells induced by arsenite treatment. J Proteome Res. 2010; 9:1129–1137. [PubMed: 20050688]

15. Heiniger HJ, Marshall JD. Cholesterol synthesis in polyclonally activated cytotoxic lymphocytes and its requirement for differentiation and proliferation. Proc Natl Acad Sci USA. 1982; 79:3823–3827. [PubMed: 6954525]
16. Brown GD. The biosynthesis of steroids and triterpenoids. Nat Prod Rep. 1998; 15:653–696.
17. Watanabe M, Yanagisawa J, Kitagawa H, Takeyama K, Ogawa S, Arao Y, Suzawa M, Kobayashi Y, Yano T, Yoshikawa H, Masuhiro Y, Kato S. A subfamily of RNA-binding DEAD-box proteins acts as an estrogen receptor alpha coactivator through the N-terminal activation domain (AF-1) with an RNA coactivator, SRA. EMBO J. 2001; 20:1341–1352. [PubMed: 11250900]
18. Yan Y, Skliris GP, Penner CC, Chooniedass-Kothari S, Cooper C, Nugent Z, Fristenski A, Hamedani MK, Blanchard A, Myal Y, Murphy LC, Leygue E. Steroid receptor RNA activator protein (SRAP): A potential new prognostic marker for estrogen receptor-positive/node-negative/younger breast cancer patients. Cancer Res. 2009; 69:597S–597S.
19. Jakob F, Tony HP, Schneider D, Thole HH. Immunological detection of the oestradiol receptor protein in cell lines derived from the lymphatic system and the haematopoietic system: variability of specific hormone binding *in vitro*. 1992; 134:397–404.
20. Roy D, Liehr JG. Estrogen, DNA damage and mutations. Mutat Res-Fundam Mol Mech Mutagen. 1999; 424:107–115.
21. Fabian CJ, Kimler BF. Selective estrogen-receptor modulators for primary prevention of breast cancer. J Clin Oncol. 2005; 23:1644–1655. [PubMed: 15755972]
22. Kumar AS, Benz CC, Shim V, Minami CA, Moore DH, Esserman LJ. Estrogen receptor-negative breast cancer is less likely to arise among lipophilic statin users. Cancer Epidemiol Biomarkers Prev. 2008; 17:1028–1033. [PubMed: 18463402]
23. Supuran CT, Scozzafava A. Carbonic anhydrases as targets for medicinal chemistry. Bioorg Med Chem. 2007; 15:4336–4350. [PubMed: 17475500]
24. Leppilampi M, Koistinen P, Savolainen ER, Hannuksela J, Parkkila AK, Niemela O, Pastorekova S, Pastorek J, Waheed A, Sly WS, Parkkila S, Rajaniemi H. The expression of carbonic anhydrase II in hematological malignancies. Clin Cancer Res. 2002; 8:2240–2245. [PubMed: 12114426]
25. Arellano R, Grinstein S. Role of isoprenylation in intracellular pH regulation of granulocytes. FEBS Lett. 1993; 332:247–250. [PubMed: 8405466]
26. Li XJ, Alvarez B, Casey JR, Reithmeier RAF, Fliegel L. Carbonic anhydrase II binds to and enhances activity of the Na+/H+ exchanger. J Biol Chem. 2002; 277:36085–36091. [PubMed: 12138085]
27. Gonzalez-Begne M, Nakamoto T, Nguyen HV, Stewart AK, Alper SL, Melvin JE. Enhanced formation of a HCO3- transport metabolon in exocrine cells of Nhe1(−/−) mice. J Biol Chem. 2007; 282:35125–35132. [PubMed: 17890222]
28. Lee KH, Finnigan-Bunick C, Bahr J, Bunick D. Estrogen regulation of ion transporter messenger RNA levels in mouse efferent ductules are mediated differentially through estrogen receptor (ER) alpha and ER beta. Biol Reprod. 2001; 65:1534–1541. [PubMed: 11673272]
29. Leese MP, Leblond B, Smith A, Newman SP, Di Fiore A, De Simone G, Supuran CT, Purohit A, Reed MJ, Potter BVL. 2-Substituted estradiol bis-sulfamates, multitargeted antitumor agents: synthesis, in vitro SAR, protein crystallography, and in vivo activity. 2006; 49:7683–7696.
30. Nilsson CL, Dillon R, Devakumar A, Shi SDH, Greig M, Rogers JC, Krastins B, Rosenblatt M, Kilmer G, Major M, Kaboord BJ, Sarracino D, Rezai T, Prakash A, Lopez M, Ji YJ, Priebe W, Lang FF, Colman H, Conrad CA. Quantitative Phosphoproteomic Analysis of the STAT3/IL-6/HIF1 alpha Signaling Network: An Initial Study in GSC11 Glioblastoma Stem Cells. J Proteome Res. 2010; 9:430–443. [PubMed: 19899826]
31. Kitoh T, Kubota M, Takimoto T, Hashimoto H, Shimizu T, Sano H, Akiyama Y, Mikawa H. Metabolic basis for differential glutamine requirements of human leukemia cell lines. J Cell Physiol. 1990; 143:150–153. [PubMed: 1969419]
32. Tsai HI, Tsai LH, Chen MY, Chou YC. Cholesterol deficiency perturbs actin signaling and glutamate homeostasis in hippocampal astrocytes. Brain Res. 2006; 1104:27–38. [PubMed: 16828067]
33. Siitonen T, Alaruikka P, Mantymaa P, Savolainen ER, Kavanagh TJ, Krejsa CM, Franklin CC, Kinnula V, Koistinen P. Protection of acute myeloblastic leukemia cells against apoptotic cell

death by high glutathione and gamma-glutamylcysteine synthetase levels during etoposide-induced oxidative stress. Ann Oncol. 1999; 10:1361–1367. [PubMed: 10631466]

34. Glickman MH, Ciechanover A. The ubiquitin-proteasome proteolytic pathway: Destruction for the sake of construction. Physiol Rev. 2002; 82:373–428. [PubMed: 11917093]

Synopsis

We assessed quantitatively the lovastatin-induced perturbation of global protein expression in HL-60 cells, and found that 122 proteins exhibited significantly altered expression. Particularly, lovastatin induced the down-regulation of important proteins in ER signaling, i.e., ERα and SRA. Additionally, the diminished expression of CAII and the resultant decrease in NHE expression induced by lovastatin may give rise to DNA degradation and cell growth inhibition. These may constitute novel mechanisms for lovastatin-induced cytotoxic effect in HL-60 cells.

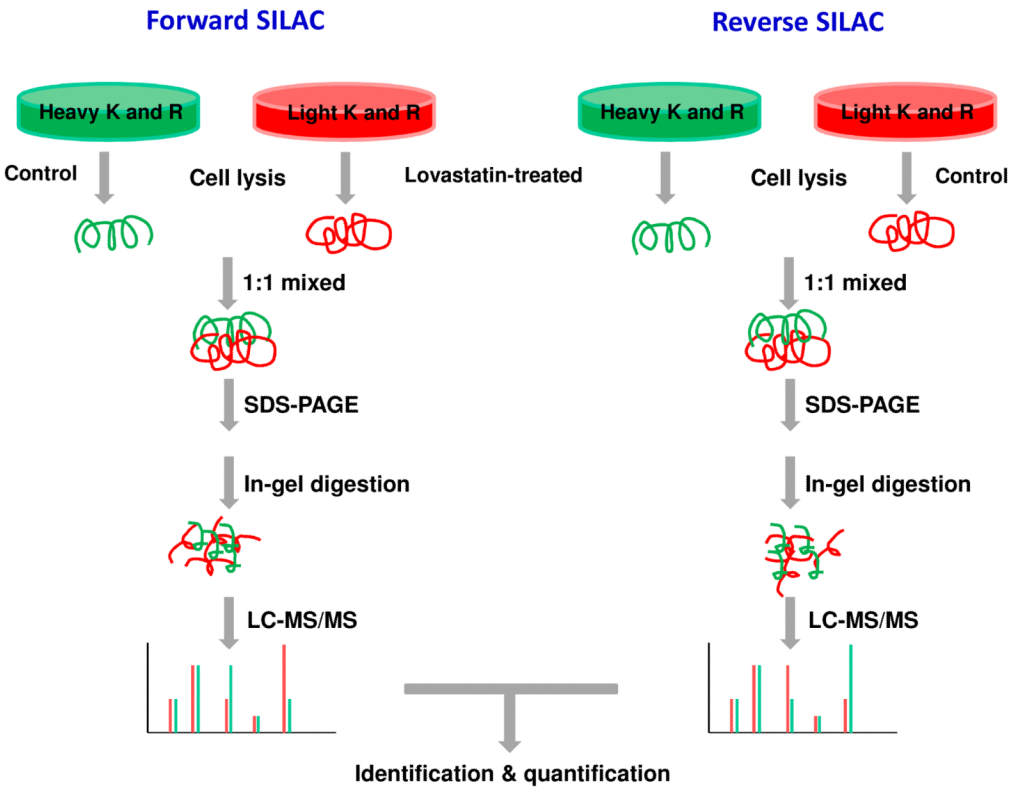

Figure 1.
Flowchart of forward and reverse SILAC coupled with LC-MS/MS for the comparative analysis of protein expression in HL-60 cells upon lovastatin treatment.

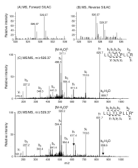

Figure 2.

Representative ESI-MS and MS/MS data revealing the lovastatin-induced down-regulation of ERα. Shown are the MS for the $[M+2H]^{2+}$ ions of ERα peptide LLLTLPLLR and LLLTLPLLR* ('R*' designates the heavy arginine) from the forward (A) and reverse (B) SILAC experiments. Depicted in (C) and (D) are the MS/MS for the $[M+2H]^{2+}$ ions of LLLTLPLLR and LLLTLPLLR*, respectively.

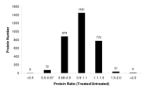

Figure 3.
The distribution of expression ratios (treated/untreated) for the quantified proteins

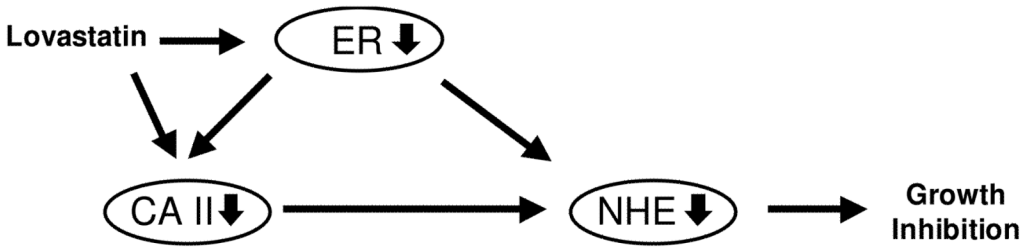

Figure 4.
Relationship between ER, CAII and NHE.

Table 1

Proteins quantified with more than 1.5 fold changes, with IPI numbers, protein names, average ratios and S.D. listed. (Other information including peptides number, sequence coverage and p-value was listed in Table S1.)

IPI Number	Protein Name	Ratio (treated/untreated)
A. Histones and hnRNPs		
IPI00455457	Histone H3	1.57 ± 0.08
IPI00807545	Herogeneous nuclear ribonucleoprotein K	1.61 ± 0.09
B. translation related factors		
IPI00014263	Eukaryotic translation initiation factor 4H	0.63 ± 0.14
IPI00925413	EIF4G1 protein	0.67 ± 0.13
IPI00290460	eIF3 p42	0.69 ± 0.06
C. Enzymes		
IPI00218414	Carbonate dehydratase II	0.17 ± 0.01
IPI00877726	Acidic-type mitochondrial creatine kinase	0.19 ± 0.05
IPI00010130	Glutamine synthetase	0.38 ± 0.13
IPI00006957	Dehydrogenase/reductase SDR family member 7	0.42 ± 0.02
IPI00021167	Interferon-inducible double stranded RNA-dependent protein kinase activator A	0.53 ± 0.03
IPI00328170	Mannosyl-oligosaccharide glucosidase	0.56 ± 0.01
IPI00221108	Thymidylate synthase	0.58 ± 0.09
IPI00008475	3-hydroxy-3-methylglutaryl coenzyme A synthase	0.58 ± 0.39
IPI00065671	Cytidine monophosphokinase 2	0.63 ± 0.01
IPI00020944	Farnesyl-diphosphate farnesyltransferase	0.64 ± 0.01
IPI00006937	Non-canonical ubiquitin-conjugating enzyme 1	0.67 ± 0.11
IPI00027851	CDNA FLJ53927, highly similar to β-hexosaminidase α chain (EC 3.2.1.52)	0.63 ± 0.07
IPI00399307	Prolylcarboxypeptidase (Angiotensinase C), isoform CRA_b	1.53 ± 0.06
IPI00306325	Protein tyrosine phosphatase, receptor type, C	1.52 ± 0.04
IPI00797038	CDNA FLJ50710, highly similar to Phosphoenolpyruvate carboxykinase (GTP), mitochondrial (EC 4.1.1.32)	1.53 ± 0.03
IPI00293564	3-hydroxy-3-methylglutarate-CoA lyase	1.54 ± 0.05
IPI00329185	1-phosphatidylinositol-4,5-bisphosphate phosphodiesterase γ-2	1.54 ± 0.04
IPI00221224	Alanyl aminopeptidase	1.56 ± 0.71
IPI00290684	2'(3')-polynucleotidase	1.58 ± 0.03
IPI00012426	Retinoid-inducible serine carboxypeptidase	1.71 ± 0.75
IPI00023728	Conjugase	1.77 ± 0.71
IPI00020632	Argininosuccinate synthase	2.19 ± 0.24
IPI00236556	84 kDa myeloperoxidase	4.03 ± 0.35
D. Others		
IPI00418471	Vimentin	0.25 ± 0.09
IPI00010341	Bone marrow proteoglycan	0.26 ± 0.04
IPI00645608	Interferon regulatory factor 2-binding protein 1	0.49 ± 0.06
IPI00027933	Low molecular mass protein 10	0.50 ± 0.05
IPI00000686	Probable RNA-binding protein 19	0.51 ± 0.09
IPI00018236	Cerebroside sulfate activator protein	0.52 ± 0.01

IPI Number	Protein Name	Ratio (treated/untreated)
IPI00023087	Cell proliferation-inducing gene 50 protein	0.52 ± 0.07
IPI00419595	Endoglycan	0.53 ± 0.06
IPI00006377	Proteasome maturation protein	0.55 ± 0.07
IPI00005670	Cell division cycle protein 123 homolog	0.55 ± 0.09
IPI00002135	ERIC-1	0.56 ± 0.12
IPI00306749	Human lung cancer oncogene 3 protein	0.56 ± 0.05
IPI00784161	Tat-cotransactivator 2 protein	0.56 ± 0.06
IPI00924510	Putative uncharacterized protein RIF1	0.56 ± 0.12
IPI00795267	Gametocyte-specific factor 1	0.56 ± 0.08
IPI00303753	Hcp β-lactamase-like protein C1orf163	0.56 ± 0.12
IPI00856042	Leucine-rich repeat-containing protein 58	0.57 ± 0.03
IPI00296259	Endoplasmic reticulum stress-response protein 25	0.58 ± 0.07
IPI00031647	Programmed cell death protein 2-like	0.59 ± 0.09
IPI00012788	A34.5	0.59 ± 0.11
IPI00031801	Cold shock domain-containing protein A	0.59 ± 0.11
IPI00306043	CLL-associated antigen KW-14	0.60 ± 0.09
IPI00002214	Importin subunit α-2	0.60 ± 0.06
IPI00043565	Coiled-coil domain-containing protein 16	0.61 ± 0.08
IPI00143753	140 kDa Ser/Arg-rich domain protein	0.61 ± 0.08
IPI00297169	Lymphocyte cytosolic protein 2	0.61 ± 0.06
IPI00384180	Dopamine receptor-interacting protein 3	0.61 ± 0.04
IPI00298935	JmjC domain-containing histone demethylation protein 2B	0.61 ± 0.10
IPI00006442	Coilin	0.61 ± 0.20
IPI00798034	Protein KRI1 homolog	0.61 ± 0.09
IPI00022386	ATP-binding protein associated with cell differentiation	0.62 ± 0.05
IPI00007004	Ribosomal RNA-processing protein 15	0.62 ± 0.11
IPI00171127	Ubiquitin-associated protein 2	0.62 ± 0.14
IPI00003318	Protein FON	0.62 ± 0.05
IPI00291930	Clathrin interactor 1	0.62 ± 0.05
IPI00008490	Protein unc-93 homolog B1	0.62 ± 0.02
IPI00006176	Hepatocyte growth factor-regulated tyrosine kinase substrate	0.62 ± 0.10
IPI00103064	Exocyst complex component 7	0.62 ± 0.06
IPI00100247	Thioredoxin domain-containing protein 13	0.63 ± 0.01
IPI00465288	Finger protein in nuclear bodies	0.63 ± 0.11
IPI00024167	ABT1-associated protein	0.63 ± 0.08
IPI00221035	RNA polymerase B transcription factor 3	0.63 ± 0.03
IPI00027180	CAAX prenyl protease 1 homolog	0.63 ± 0.05
IPI00007729	Nucleolar protein 7	0.64 ± 0.05
IPI00647185	Centrosomal protein 170kDa	0.64 ± 0.09
IPI00020961	Apoptosis regulator Bcl-2	0.64 ± 0.05
IPI00009005	Activating enhancer-binding protein 4	0.64 ± 0.04
IPI00218829	G1 to S phase transition protein 1 homolog	0.64 ± 0.01

IPI Number	Protein Name	Ratio (treated/untreated)
IPI00004233	Antigen KI-67	0.64 ± 0.05
IPI00015808	Autoantigen NGP-1	0.65 ± 0.12
IPI00018192	NOP seven-associated protein 1	0.65 ± 0.03
IPI00028481	Oncogene c-mel	0.65 ± 0.05
IPI00470779	α-taxilin	0.65 ± 0.1
IPI00384541	Regulation of nuclear pre-mRNA domain-containing protein 2	0.65 ± 0.06
IPI00217686	Protein ftsJ homolog 3	0.65 ± 0.15
IPI00215768	γ-glutamylcysteine synthetase	0.65 ± 0.07
IPI00514856	Protein NICE-4	0.65 ± 0.2
IPI00185919	La ribonucleoprotein domain family member 1	0.65 ± 0.16
IPI00005717	Estrogen-related receptor α	0.66 ± 0.06
IPI00889000	Neurochondrin	0.66 ± 0.10
IPI00432363	Microtubule-actin cross-linking factor 1, isoform 4	0.66 ± 0.14
IPI00412415	ATP-dependent chromatin-remodeling protein	0.67 ± 0.04
IPI00291064	AN1-type zinc finger protein 1	0.67 ± 0.12
IPI00219168	β-V spectrin	0.67 ± 0.05
IPI00012773	Metastasis-associated protein MTA1	0.67 ± 0.17
IPI00001960	Chloride intracellular channel protein 4	1.50 ± 0.35
IPI00024971	Oxysterol-binding protein 1	1.51 ± 0.11
IPI00033153	mRNA export factor TAP	1.51 ± 0.08
IPI00015148	GTP-binding protein smg p21B	1.52 ± 0.03
IPI00878557	δ transcription factor	1.54 ± 0.05
IPI00219219	14 kDa laminin-binding protein	1.54 ± 0.36
IPI00394994	Nesprin-3	1.55 ± 0.02
IPI00103483	Cofactor of BRCA1	1.56 ± 0.07
IPI00017289	Nucleic acid-binding protein RY-1	1.57 ± 0.73
IPI00020075	Abhydrolase domain-containing protein 10, mitochondrial	1.57 ± 0.08
IPI00009368	Sideroflexin-1	1.57 ± 0.11
IPI00793723	CDK7/cyclin-H assembly factor	1.61 ± 0.10
IPI00848090	cDNA, FLJ94534, highly similar to Homo sapiens capping protein (actin filament), gelsolin-like(CAPG), mRNA	1.64 ± 0.04
IPI00903062	cDNA FLJ43948 fis, clone TESTI4014924, highly similar to cytoplasmic FMR1 interacting protein 1 (CYFIP1), transcript variant 1, mRNA	1.66 ± 0.13
IPI00478758	UPF0557 protein C10orf119	1.69 ± 0.07
IPI00007812	Endomembrane proton pump 58 kDa subunit	1.70± 0.27
IPI00922511	cDNA FLJ54854, highly similar to junctional adhesion molecule A	1.71 ± 0.30
IPI00478231	Rho cDNA clone 12	1.94 ± 0.24
IPI00410067	Zinc finger antiviral protein	1.99 ± 0.30
IPI00295940	cDNA FLJ55508, highly similar to Sad1/unc-84-like protein 2	1.99 ± 0.74
IPI00007061	Golgi transport 1 homolog B	2.18 ± 0.30
IPI00397229	CD97 antigen	2.25 ± 0.27
IPI00071826	cDNA FLJ55391	2.53 ± 0.10
IPI00021812	Desmoyokin	2.55 ± 0.30

IPI Number	Protein Name	Ratio (treated/untreated)
IPI00418169	Annexin A2	2.56 ± 0.96
IPI00032313	Calvasculin	2.67 ± 0.28
IPI00847793	Dermcidin isoform 2	2.69 ± 0.08
IPI00375156	Putative neutrophil cytosol factor 1B	3.31 ± 0.75
IPI00386208	Drug-sensitive protein 1	9.56 ± 6.28

Table 2

Pathways perturbed by lovastatin treatment, as identified by IPA.

Ingenuity Canonical Pathways	Proteins
Estrogen Receptor Signaling	TAF9, SRA, general transcription factor TFIIB, MED1, MED12
Glutamate Metabolism	GS, γ-ECS
Protein Ubiquitination Pathway	BIRC6, USP10, DNAJC2, UBE2S, UBE2J1, HLA-C
Cholesterol Biosynthesis	HMGCS, FDFT1
EIF2 Signaling	EIF3G, EIF4G1, EIF2A